Biometals (2010) 23:669–680
DOI 10.1007/s10534-010-9327-z

Exposure to lanthanum compound diminishes LPS-induced inflammation-associated gene expression: involvements of PKC and NF-κB signaling pathways

Fei Guo · Yuanlei Lou · Nianhua Feng · Guohui Li · An Xie · Xueming Huang · Yang Wang

Received: 7 December 2008 / Accepted: 11 March 2010 / Published online: 27 March 2010

Abstract Lanthanum chloride, a rare earth compound, possesses antibacterial and cellular immunity regulating properties. However, the underlying molecular mechanisms remain largely unknown. In this study, we examined the effects of lanthanum chloride on the production of nitric oxide (NO) and tumor necrosis factor-α (TNF-α), the expression of inducible NO synthase (iNOS) and TNF-α in RAW 264.7 cells, a mouse macrophage cell line. We found that the LPS-elicited excessive production of NO and TNF-α in RAW 264.7 cells was inhibited significantly in the presence of lanthanum chloride, and the attenuation of iNOS and TNF-α occurred at mRNA level. Furthermore, the possible signaling components affected by lanthanum chloride in the pathway that lead to LPS-induced iNOS and TNF-α expression were explored. The results indicated the involvements of PKC/Ca^{2+} and NF-κB in the attenuation of NO and pro-inflammatory cytokine production by lanthanum chloride. Our observations suggest a possible therapeutic application of this agent for treating inflammatory diseases.

Keywords Lanthanum chloride · Inducible nitric oxide synthase (iNOS) · Tumor necrosis factor-α (TNF-α) · Nuclear factor-κ B (NF-κ B) · Protein kinase C (PKC)

Introduction

Macrophages produce molecules such as nitric oxide (NO) and tumor necrosis factor-α (TNF-α), which are known to play roles in inflammatory responses. Excessive production of NO and pro-inflammatory cytokines by activated macrophages plays an important role in the pathogenesis of various inflammatory diseases such as septic shock and rheumatoid arthritis. Therefore, proper control of macrophage activity is an important strategy in the treatment of inflammatory diseases.

The study of mechanisms of signal transduction cascades involved in the induction of inducible nitric oxide synthase (iNOS) and cytokines in response to lipopolysaccharide (LPS, endotoxin) is an active area of investigation. Nuclear factor-κ B (NF-κB) appears to play a key role in the transcriptional regulation of iNOS and TNF-α expressions (Chen et al. 1995).

F. Guo · G. Li
Burns Institute, The First Affiliated Hospital of Nanchang University, Nanchang 330006, People's Republic of China

Y. Lou · N. Feng · A. Xie · X. Huang · Y. Wang (✉)
Institute of Urology, The First Affiliated Hospital of Nanchang University, Nanchang 330006, People's Republic of China
e-mail: wangy63cn@126.com

NF-κB belongs to a ubiquitous family of transcription factors present in the cell cytoplasm; these proteins are bound to IκB, which belongs to a family of structurally related inhibitor proteins. Appropriate stimulation phosphorylates IκB on specific serine residues and targets it for degradation by proteasome; subsequently, NF-κB is translocated into the nucleus where it activates the transcription of the target genes (Ghosh and Karin 2002; Nelson et al. 2004).

Several studies have suggested that the protein kinase C (PKC) pathway, involving a family of structurally related, phospholipid-dependent, serine-threonine kinases (Hofmann 1997; Parker and Murray-Rust 2004), is also one of the main signal transduction systems involved in inflammatory responses (Parker and Murray-Rust 2004; Severn et al. 1992; Spitaler and Cantrell 2004). Several lines of evidence suggest that PKCs are involved in LPS- and cytokine-induced expression of inflammatory genes, including iNOS (Oh et al. 2007). Furthermore, many studies suggest that PKC/Ca^{2+} plays an important role in the activation of NF-κB in response to infectious agents and other stimuli. Consistently, in vitro studies have indicated that activated PKC alone can induce NF-κB activation (Lallena et al. 1999; Ogata et al. 2000; Trushin et al. 2003).

It has been reported that in vivo administration of gadolinium chloride ($GdCl_3$) to rats decreases the NO release and iNOS expression by isolated rat Kupffer cells after treatment with LPS (Roland et al. 1996). Further, $GdCl_3$ pretreatment eliminated the LPS-induced increase in iNOS activity and protein expression in the lungs and significantly lowered the levels of exhaled pulmonary NO (Fujii et al. 1998). Lanthanide ions have been proven to possess various biologic effects (Dai et al. 2008a, b; Hu et al. 2006; Manolov et al. 2006; Shigematsu 2008). Gadolinium and lanthanum, which are trivalent cations belonging to the group of lanthanide elements, possess antibacterial and cellular immunity-regulating properties; however, the metabolism, tissue deposition, and clinical uses of lanthanum and gadolinium are remarkably different (De Broe 2008). Gadolinium is a heavy metal while lanthanum is a light rare-earth element whose toxicity is as low as that of iron (Qin et al. 2002). Lanthanide compounds have been employed in the treatment of various diseases. For example, lanthanum carbonate is well tolerated and effective for the long-term maintenance of serum phosphorus control in patients with end-stage renal disease (Chiang et al. 2005; Shigematsu 2008). Studies have also shown that a combination treatment of sulfadiazine and cerium nitrate is efficient in the treatment of burn patients (de Gracia 2001; Deveci et al. 2000; Hadjiiski and Lesseva 1999). We have previously reported that lanthanum chloride can reduce LPS toxicity, inhibit LPS-induced apoptosis of thymocytes, and prevent LPS-induced liver and lung damage; in addition, it markedly decreases the plasma level of TNF-α and TNF-α mRNA expression in mice challenged with LPS, thus protecting the mice treated with lethal doses of LPS (Wang et al. 2004). However, the mechanism by which lanthanum ion modulates LPS-mediated inflammatory response remains largely unknown. In this study, we investigated whether lanthanum chloride attenuates the excessive production of NO and the pro-inflammatory cytokine, TNF-α, and the underlying mechanisms in LPS-stimulated RAW 264.7 cells belonging to a mouse macrophage cell line. We found that the LPS-elicited excessive production of NO and TNF-α in RAW 264.7 cells was largely inhibited in the presence of lanthanum chloride, and the attenuation of iNOS and TNF-α activities resulted from their reduced mRNA expressions. Further, we investigated the cell signaling pathways involved in lanthanum chloride inhibition of LPS-induced iNOS and TNF-α expression. The results of our study indicate that PKC/Ca^{2+} and NF-κB pathways are involved in the attenuation of NO and pro-inflammatory cytokine production by lanthanum chloride.

Materials and methods

Cell culture

The RAW 264.7 mouse macrophage cell line, obtained from the Committee on Type Culture Collection of Chinese Academy of Sciences, was maintained in Dulbecco's modified eagle medium/HamF12 (DMEM-F12; LPS < 0.03 U/ml; Hyclone) supplemented with 5% heat-inactivated fetal bovine serum (FBS) (Gibco) under a humidified atmosphere of 5% CO_2/95% air. Before each experiment, cells were plated in 24-well plates and/or culture flasks at a density of 2×10^5 cells/ml for analyzing the

supernatant or for protein extraction and RNA extraction. Interference from FBS (FBS may bind with LPS and/or lanthanum chloride) was prevented by washing the cells 3 times with DMEM-F12 before incubation with lanthanum, and subsequently fresh DMEM-F12, rather than DMEM-F12 containing 5% FBS, was added to the wells or flasks. The cells were pre-treated with lanthanum chloride ($LaCl_3 \cdot 7H_2O$; purity, 99.9%; Sigma) for the time indicated in the figures, washed 3 times with DMEM-F12, and stimulated with LPS (serotype 055:B5; 1 μg/ml; Sigma) for the indicated time.

Assay for the determination of cell viability

Cell respiration, which is an indicator of cell viability, was analyzed on the basis of the mitochondrial-dependent reduction of 3-(4,5-dimethylthiazol-2-yl)-2,5-diphenyltetrazolium-bromide (MTT) to formazan. RAW 264.7 cells were cultured in 96-well plates (1×10^5 cells/ml) for 24 h. The cells were pretreated with various concentrations (0, 100, 500, and 2500 nM) of lanthanum chloride, washed 3 times, and stimulated by LPS (1 μg/ml). After overnight incubation, the cells were washed once and subsequently, 100 μl of FBS-free medium containing 5 mg/ml of MTT was added. After 24 h of incubation at 37°C, the medium was discarded and the formazan blue formed in the cells was dissolved in 100 ml of dimethyl sulfoxide (DMSO). The optical density of the solution was measured at 570 nm, and the cytotoxicity of various lanthanum chloride concentrations was evaluated; if the optical density value of the lanthanum chloride treated groups achieves a 20% reduction compared to that of the untreated group, the concentration of the lanthanum chloride was considered to be cytotoxic.

NO release assay

NO production in the culture supernatant was determined by the nitrate reductase assay. Cells were treated with 0–2500 nM of lanthanum chloride for 24 h, washed 3 times, and then stimulated with LPS (1 μg/ml) for 24 h. The supernatants were collected and analyzed for NO production using the nitrate reductase kit (Jingmei Biotech Co., Ltd., China). The OD value at 540 nm was determined by a spectrophotometer (DU640; Beckman, USA) and NO concentrations were calculated using the following formula: NO (μM) = $A_{sample}/A_{standard} \times 100$ (μM).

Measurement of TNF-α Release

The TNF-α level was assessed by enzyme-linked immunosorbent assay (ELISA) using monoclonal antibodies, according to the procedure recommended by the supplier (eBiosciences). The cells were treated with 0–2500 nM of lanthanum chloride for 2 h, washed, and subsequently stimulated with LPS (1 μg/ml) for 4 h. The supernatants were collected and TNF-α expression was analyzed by ELISA. The concentration of TNF-α was calculated according to the standard curve provided in the ELISA kits.

Immunofluorescence staining

Cells adhered to coverslips were fixed with freshly prepared 3% paraformaldehyde for 15 min and permeabilized with 0.5% Triton X-100 for 15 min. Non-specific binding was reduced by blocking the cells with 1% bovine serum albumin (BSA) for 30 min at 37°C, and then incubation for 2 h with goat anti-p-PKC α (Santa Cruz, CA, USA) or mouse anti-NF-κB/p65 (Santa Cruz, CA, USA) antibodies diluted at 1:100 in phosphate-buffered saline (PBS) containing 1% BSA. The cells were subsequently washed, incubated with FITC-conjugated IgG (Sigma, USA) at 1:100 for 1 h, and then washed again. In the NF-κB/p65 assay, the nuclei were identified by counterstaining the samples with 4′,6-diamidino-2-phenylindole (DAPI) (Sigma, USA) and subsequently, images were obtained using a fluorescence microscope (IX71, equipped with DP70 high sensitivity digital color camera; Olympus, Japan).

Cytosolic Ca^{2+} measurements

The intracellular Ca^{2+} ($[Ca^{2+}]_i$) was determined using Fluo-3/acetoxymethyl ester (Fluo-3/AM, Molecular Probes, Eugene, Oregon, USA), described previously with slight modification (Kao et al. 1989; Sudhandiran and Shaha 2003; Zhu et al. 2006). Briefly, RAW 264.7 macrophages were loaded for 30 min at 25°C with 5 μM Fluo-3/AM containing 1 μM pluronic acid F-127 for proper dispersal and 0.25 mM sulfinpyrazone, to inhibit the leakage of the Fluo-3 dye. Shortly before use, a sample of loaded

cells was washed with Krebs–Ringer-HEPES (KRH) buffer (130 mM NaCl, 1.3 mM KCl, 2.2 mM. $CaCl_2$, 1.2 mM $MgSO_4$, 1.2 mM KH_2PO_4, 10 mM HEPES, 10 mM glucose, pH 7.4), to remove nonhydrolyzed Fluo-3/AM. Fluorescence measurements were performed at 25°C with excitation at 488 nm and emission at 526 nm using flow cytometer (FACSCalibur, Becton–Dickinson). To convert fluorescence values into absolute $[Ca^{2+}]_i$, calibration was performed at the end of each experiment. $[Ca^{2+}]_i$ was calculated using the equation: $[Ca^{2+}]_i = K_d[(F - F_{min})/(F_{max} - F)]$, in which K_d is the dissociation constant of the Ca^{2+}·Fluo 3 complex (400 nM) and F represents the fluorescence intensity of the cells. F_{max} represents the maximum fluorescence (obtained by treating cells with 10 μM calcium ionophore A23187), and F_{min} corresponds to the minimum fluorescence (obtained from ionophore-treated cells in the presence of 3 mM EGTA). Fluorescence intensities were expressed as the increase in fluorescence over base-line fluorescence intensity before stimulation.

Preparation of total protein extract and RNA extracts

The total cellular protein and RNA were isolated using Takara Protein Kit and RNA Extraction Kit for Mammalian Cultured Cells, respectively (Takara, Dalian, China). The cells were washed twice with cold pyrogen-free physiologic saline, collected by centrifugation, re-suspended in cell-lysis buffer on ice for 10 min, and centrifuged at 12,000×g for 5 min, according to the instructions supplied by the manufacturer. The supernatants containing soluble cellular proteins were divided into aliquots and stored at −80°C. The protein concentrations in the extract were determined using the Bio-Rad protein assay kit. Next, RNA extracts were prepared by adding a denaturation solution to the abovementioned aliquots in a 3:1 ratio; the samples were then incubated with isopropanol for 10 min at room temperature and centrifuged at 12,000×g for 15 min at 4°C. After washing with 80% alcohol, the samples were centrifuged at 12,000×g for 5 min at 4°C. The precipitates were then dissolved in RNA preparation water provided by the manufacturer and the A_{260}/A_{280} value of the samples was determined by Nucleic and Protein Analyzer (DU640; Beckman, USA).

Preparation of cytoplasmic and nuclear fractions

Cytoplasmic and nuclear extracts were prepared using the nuclear extract kit (Active Motif, USA) according to the instructions given in the manual. Briefly, 8.8×10^6 cells were washed with ice-cold PBS containing phosphatase inhibitors, gently re-suspended in 500 μl of hypotonic buffer, and incubated for 15 min. Next, 25 μl detergent was added and the suspension was vortexed for 10 s at the highest speed and then centrifuged for 30 s at 14,000×g in a microcentrifuge precooled to 4°C. The supernatant (cytoplasmic fraction) was transferred into a prechilled microcentrifuge tube and stored in aliquots at −80°C until ready to use. Subsequently, the nuclear pellet was re-suspended in 50 μl of complete lysis buffer and the suspension was incubated for 30 min on ice on a rocking platform set at 150 rpm. After 30 s, the sample was vortexed at the highest speed; the suspension was centrifuged for 10 min at 14,000×g in a microcentrifuge precooled to 4°C. The supernatant (nuclear fraction) was also transferred into a prechilled microcentrifuge tube and stored in aliquots at −80°C until ready to use. The protein concentration was determined by the Bio-Rad protein assay reagent according to the manufacturer's instructions.

Reverse transcription-polymerase chain reaction

cDNA was obtained from the total RNA (1 μg/sample) using a reverse transcription kit, according to the manufacture's instructions. Then, the expression of iNOS, TNF-α, and β-actin (as the internal standard) in the cDNA aliquots was determined by performing polymerase chain reaction (PCR) with a thermal cycler (Biometra, Germany). All PCR amplifications were performed using the recommended buffer that was supplied by the manufacturer. The PCR mixture contained 2 μl of each template and 0.05 μM of each primer. The reactions were performed in triplicate for each template. After initial denaturation for 2 min at 95°C, 36 amplification cycles were performed for iNOS (30 s at 95°C, denaturation; 45 s at 69°C, annealing; and 45 s at 72°C, extension) and 21 cycles were performed for TNF-α (30 s at 95°C, denaturation; 45 s at 60°C, annealing; and 45 s at 72°C, extension). We used the following PCR primers from Bio Basic Inc.

(Shanghai, China): iNOS, sense strand: 5′-GTT TCT GGC AGC GGC TC-3′ and anti-sense strand: 5′-GCT CCT CGC TCA AGT TCA GT-3′ (Nahrevanian and Dascombe 2002); β-actin, sense strand: 5′-CGT GGG CCG CCC TAG GCA CCA GGG-3′ and anti-sense strand 5′-GGG AGG AAG AGG ATG CGG CAG TGG-3′ (Wolfs et al. 2002); and TNF-α, sense strand 5′-GGC AGG TCT ACT TTG GAG TCA TTG C-3′ and anti-sense strand 5′-ACA TTC GAG GCT CCA GTG AAT TCG G-3′ (Wang et al. 2004). After amplification, the PCR products were analyzed by electrophoresis on a 2% agarose gel, and visualized under an ultraviolet transilluminator by ethidium bromide staining and photographed. The optical density (OD) of the iNOS, TNF-α, and β-actin bands was measured by a digital imaging system (Image-Quant™ 300; GE Healthcare Life Science). The mRNA levels of iNOS and TNF-α were normalized against those of β-actin.

Western blot analysis

The proteins in the total protein extract were separated (30 μg/lane) by 10% sodium dodecyl sulfate-polyacrylamide gel electrophoresis (SDS-PAGE) and transferred onto nitrocellulose membranes by using a semi-dry blotter (BIO-RAD, USA). The membranes were incubated overnight with Tween 20/Tris-buffered saline (TTBS) containing 5% (w/v) nonfat milk at 4°C, and subsequently with indicated dilution of primary antibody for 4 h. The blots were washed 3 times with TTBS and incubated with a 1:2000 dilution of horseradish peroxidase (HRP)-conjugated IgG secondary antibody for 1 h at room temperature. Then, the blots were washed 3 times with TTBS and visualized by enhanced chemiluminescence (Pierce, USA), followed by autoradiography. The antibodies used in this study were as follows: anti-iNOS (1:1,000; Santa Cruz, CA, USA), anti-PKCα, anti-phospho-PKC α (1:1,000; Santa Cruz, CA, USA), anti-NF-κB/p65 (1:1,000; Santa Cruz, CA, USA), and anti-β-actin (1:2,000; Sigma).

Nuclei p65 activity assay

According to a previous report (Zhang et al. 2005), NF-κB activation in the nuclear extracts can be quantified using a TransAM NF-κB assay kit (Active Motif); this method is based on the principle of ELISA. Specifically, an oligonucleotide containing the NF-κB consensus site (5′-GGGACTTTCC-3′) was immobilized on the microwell plates. The active form of NF-κB present in nuclear extracts that binds specifically to this oligonucleotide was detected using a primary antibody. Subsequently, an HRP-conjugated secondary antibody was added to the wells, and the plates were read using an automated plate reader; the expression level of nuclear NF-κB p65 was determined as absorbance at 450 nm (A_{450}).

Statistical analysis

All the experiments were independently performed at least 3 times with data presented as mean ± SD (standard deviation of the mean). Statistical analyses were performed using Student's t-test and one-way analysis of variance (ANOVA). $P < 0.05$ was considered as statistically significant.

Results

Inhibition of NO production by lanthanum chloride

We investigated the effects of lanthanum chloride on NO production in LPS-stimulated RAW 264.7 cells by treating the cells with either LPS alone or with various concentrations of lanthanum chloride for 24 h before LPS stimulation. NO production in the culture medium was determined by performing a nitrate reductase assay. Lanthanum chloride did not exhibit cytotoxic effects at any concentration used in this study, and this result was confirmed by the MTT assay (Fig. 1). Lanthanum chloride decreased the LPS-induced production of NO in RAW 264.7 cells in a dose-dependent manner (Fig. 2a). To elucidate the mechanism responsible for the inhibitory effect of lanthanum chloride on NO production, we evaluated the iNOS mRNA and protein levels by RT-PCR and western blotting, respectively. At a concentration of 2500 nM, lanthanum chloride effectively inhibited iNOS mRNA (Fig. 2b) and protein (Fig. 2c) expression in LPS-stimulated RAW 264.7 cells. These data suggest that the inhibition of NO production caused by lanthanum chloride occurred at iNOS gene transcriptional level.

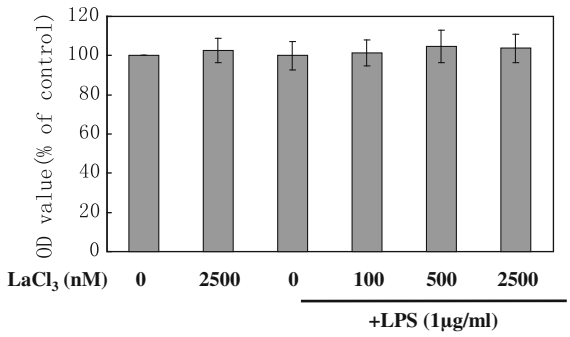

Fig. 1 Effects of lanthanum chloride on the viability of RAW 264.7 cells

Inhibition of pro-inflammatory cytokine production by lanthanum chloride

The inhibitive effect of lanthanum chloride for NO production in the macrophage cell line prompt us to check the role of this drug in regulating other pro-inflammatory mediators such as TNF-α. As shown in Fig. 3, LPS-stimulated RAW 264.7 macrophages exhibited increased TNF-α production, while pretreatment with lanthanum chloride treatment inhibited the production in a dose-dependent manner. To elucidate the mechanism responsible for the inhibitory effect of lanthanum chloride on TNF-α production, we next analyzed the TNF-α mRNA expression level by RT-PCR. Lanthanum chloride markedly decreased the mRNA levels of TNF-α in RAW 264.7 cells to a near basal level (Fig. 3a). These data suggest that lanthanum chloride might act as a modulator of the inflammatory cytokine production.

Inhibition of PKC/Ca^{2+} signaling by lanthanum chloride

Since PKC/Ca^{2+} pathways are involved in the NO production in response to LPS stimulation (Severn et al. 1992), we assessed whether the repressive effect of lanthanum chloride occurred at PKC level. As shown in Fig. 4a, FITC-labeled phospho-PKC α (p-PKC α) was mainly localized in the cell periphery, i.e., close to the cell surface. The FITC-labeled green signals of p-PKC α in LPS-treated RAW 264.7 macrophages were markedly high, while those in lanthanum chloride-treated cells were greatly attenuated. Western blotting was performed to further

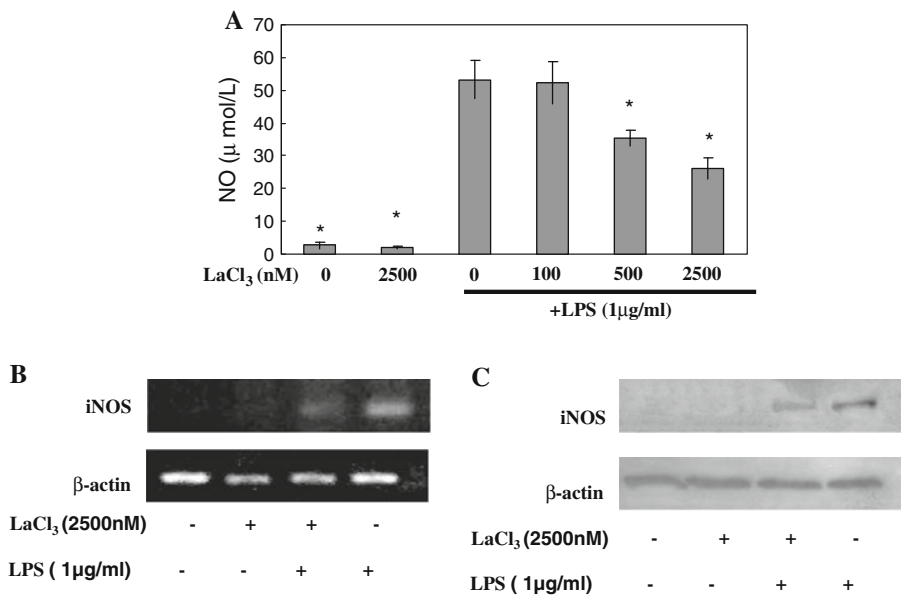

Fig. 2 Effects of lanthanum chloride on LPS-induced production of NO in RAW 264.7 cells. **a** Cells were pretreated with lanthanum chloride (0, 100, 500 and 2500 nM), washed, and then stimulated with LPS (1 μg/ml) for 24 h. The NO concentration was determined in culture medium using Nitric Oxide Assay Kit. Data represent the mean ± SD of three independent experiments. * $P < 0.01$ vs. LPS alone. **b**, **c** Cells were treated with LPS alone or pretreated with lanthanum chloride (2500 nM), washed and subsequently treated with LPS for 24 h for RT-PCR and Western blot. The mRNA expression and protein levels of iNOS were evaluated by RT-PCR and Western blot, respectively

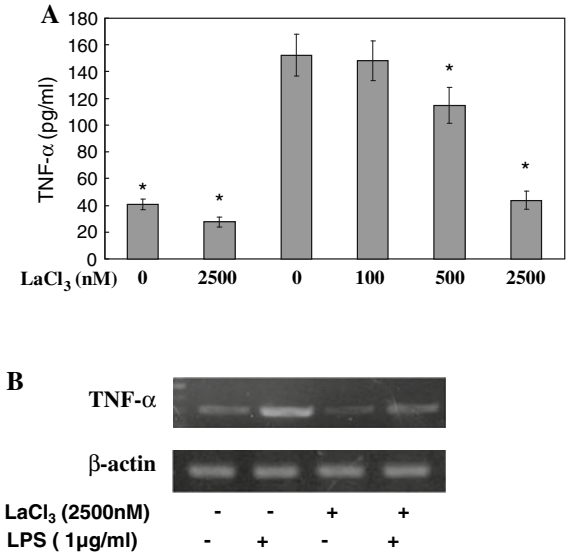

Fig. 3 Effects of lanthanum chloride on LPS-induced TNF-α in RAW 264.7 cells. Cells were pretreated with lanthanum chloride (0, 100, 500 and 2500 nM), washed and followed by 4 h LPS (1 μg/ml) stimulation for RT-PCR (**b**) and 24 h stimulation for ELISA (**a**). Each cytokine concentration was measured in culture medium using ELISA. Data represent the mean ± SD of three independent experiments. * $P < 0.01$ vs. LPS alone

examine the extent of phosphorylation of PKC α in RAW 264.7 cells (Fig. 4b). The results showed that lanthanum chloride markedly suppressed PKC α phosphorylation in LPS-stimulated macrophages. Since La^{3+} is known as one of the Ca^{2+} antagonists, we further investigated the effects of lanthanum chloride by using extracellular Ca^{2+} chelator, EGTA, as well as intracellular Ca^{2+} chelator, BAPTA-AM on $[Ca^{2+}]_i$ in RAW 264.7 macrophages induced by LPS. We found that $[Ca^{2+}]_i$ increased significantly in RAW 264.7 cells treated with LPS alone (compared with untreated control, $P < 0.01$), but decreased significantly by pretreatment of the cells with 2500 nM $LaCl_3$ for 50 s(Chang et al. 2008a), 5 mM EGTA for 5 min (Letari et al. 1991) or BAPTA/AM for 1 h (Choi et al. 2001), respectively, before 2 min-LPS stimulation (compared with LPS group, $P < 0.01$). Both $LaCl_3$ and extracellular/intracellular Ca^{2+} chelators significantly blunted the LPS-induced increase in $[Ca^{2+}]_i$ (Fig. 4c). We further explored whether the phosphorylation of PKC α could be suppressed using western blot. The results showed that the phosphorylation of PKC α was eliminated almost completely by pre-treating the cells with $LaCl_3$, BAPTA/AM or EGTA, respectively (Fig. 4d). Collectively, all these findings indicate that lanthanum chloride effectively inhibits the activation of PKC/Ca^{2+} pathways in LPS-stimulated macrophages.

Inhibition of NF-κB activation by lanthanum chloride

We next examined the influence of lanthanum chloride on NF-κB activation as potential transcription factor targeted. First, we detected the nuclear expression of NF-κB/p65 protein by immunofluorescence staining. Then, we detected the degradation of cytoplasmic IκB α and the expression of nuclear NF-κB/p65 by western blot. Finally, we assessed the DNA-binding activity of NF-κB by using TransAM NF-κB assay kit. As shown in Fig. 5, LPS-induced nuclear translocation of NF-κB/p65 was significantly reduced and the degradation of IκB α were significantly decreased after lanthanum chloride treatment; in addition, the LPS-induced DNA-binding activity of NF-κB was also suppressed significantly by lanthanum chloride, which indicated the involvement of the NF-κB pathway.

Discussion

In the present study, we examined the effects of lanthanum chloride on LPS-induced NO production and TNF-α expression in RAW 264.7 cell line. The results of our experiments indicate that lanthanum chloride is a potent inhibitor of NO and TNF-α release. Consistent with these observations, we found that lanthanum chloride also decreased the protein and mRNA levels of iNOS and TNF-α. The inhibition of the expression of these molecules in LPS-stimulated RAW 264.7 cells by lanthanum chloride did not contribute to cytotoxicity, as determined by the MTT assay and β-actin expression.

The expressions of iNOS and TNF-α in murine macrophages have been shown to be dependent on NF-κB activity (Baeuerle 1998; Xie et al. 1994). Numerous studies demonstrated that the PKC isoforms play a critical role in the activation of IκB kinase β (IKK β) and the degradation of IκB in the NF-κB pathway (Lallena et al. 1999; Moscat et al. 2003; Steffan et al. 1995; Trushin et al. 2003; Zhong

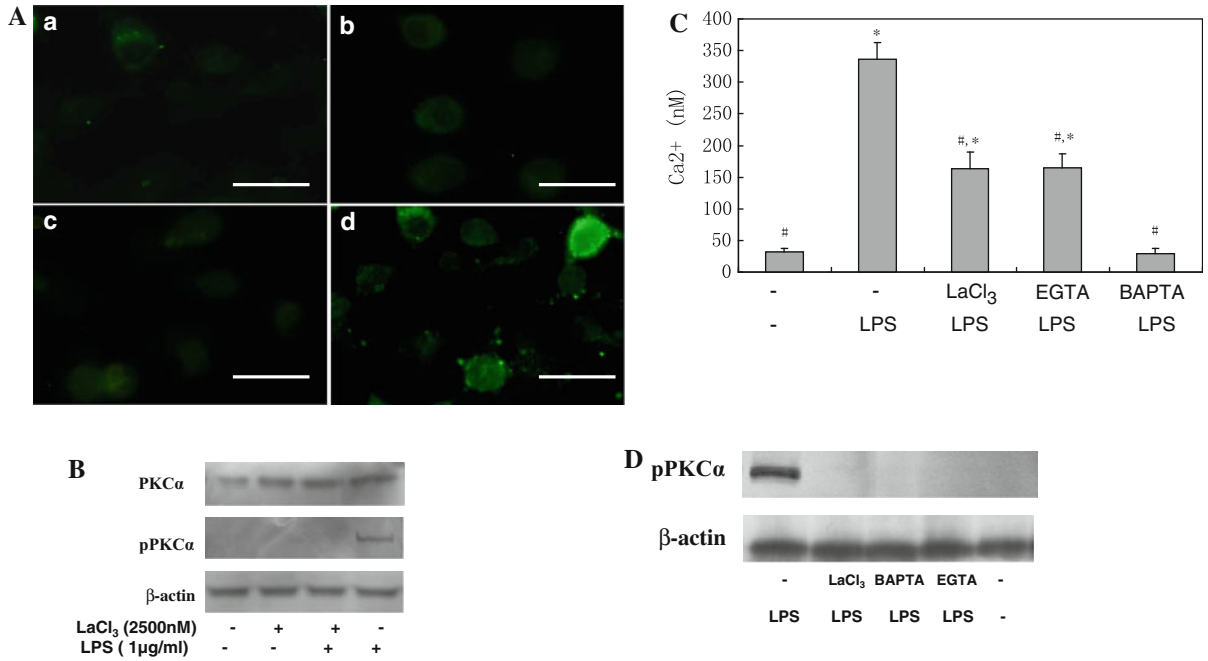

Fig. 4 Effect of Lanthanum chloride on LPS-induced phosphorylation of PKC in RAW 267.4 cells. **A** Immunofluorescent staining analysis of phosphor-PKCα: *a* control; *b* cells were treated with lanthanum chloride (2500 nM) in the absence of LPS for 10 min; *c* cells were pretreated with Lanthanum chloride (2500 nM) for 2 h, washed, and stimulated with LPS (1 μg/ml) for 10 min; *d* cells were treated with LPS (1 μg/ml) for 10 min (*Bar* = 20 μm). **B** Total cell extracts were subjected to immunoblot analysis using antibodies against phosphoror total forms of PKCα. **C** $[Ca^{2+}]_i$ in RAW 264.7 macrophages induced by LPS in the presence or absence of extracellular Ca^{2+}, intracellular Ca^{2+} or La^{3+}, respectively (n = 3, Mean ± SD). In La + LPS group, lanthanum chloride (2500 nM) was added 50 s before LPS stimulation; in EGTA + LPS group, the cells were pretreated with 5 mM EGTA for 5 min before LPS stimulation. $[Ca^{2+}]_i$, was detected 2 min after LPS treatment. In BAPTA/AM + LPS group RAW 264.7 cells pretreated with 50 μM BAPTA/AM for 1 h before LPS stimulation. # $P < 0.01$ vs. LPS group; * $P < 0.01$ vs. untreated control group. **D** The LPS-induced phosphorylation of PKCα was eliminated by pretreating the cells with lanthanum chloride, BAPTA/AM or EGTA, respectively. RAW 264.7 cells pretreated with 2500 nM lanthanum chloride for 30 min, 50 μM BAPTA/AM for 1 h or 5 mM EGTA for 5 min, respectively, pPKCα was detected in 10 min

et al. 1997). Studies also suggest that PKC α plays an important role in LPS-induced NO formation (Li et al. 1998; Lin and Chang 1996; Severn et al. 1992). In the current study, we found that lanthanum chloride inhibited LPS-induced PKC α phosphorylation and the DNA-binding activity of NF-κB, which was associated with the prevention of IκB α degradation and subsequently decreased p65 protein level in the nuclei. It has been proven that LPS triggers a cascade of intracellular signal transduction pathways involved in iNOS/TNF-α expression, including the activation of PKC, PKA, ERK, and p38 MAPK (Chen et al. 1999; Chen and Wang 1999; Hambleton et al. 1995; Li et al. 1998; Lin and Chang 1996; Sanghera et al. 1996; Zhong et al. 1997). To better understand the role of other signal pathways involved in the inhibiting effects of lanthanum chloride on LPS-mediated iNOS and TNF-α mRNA expression, we have also investigated the activation of PKA and p38 MAPK pathways. The results of these experiments showed that lanthanum did not play a role in the inhibition of LPS-mediated PKA or p38 MAPK activation (data not shown). Hence, the key molecular mechanisms underlying the lanthanum chloride-mediated attenuation of iNOS and TNF-α expression were the inhibition of LPS-induced phosphorylation of PKC and the DNA-binding activity of NF-κB.

Consistent with our present study, NF-κB activity has been reported to be affected by various metal elements. For example, gold, zinc, and copper compounds can block the activation of NF-κB by inhibiting the activity of IKKs (Jeon et al. 2003;

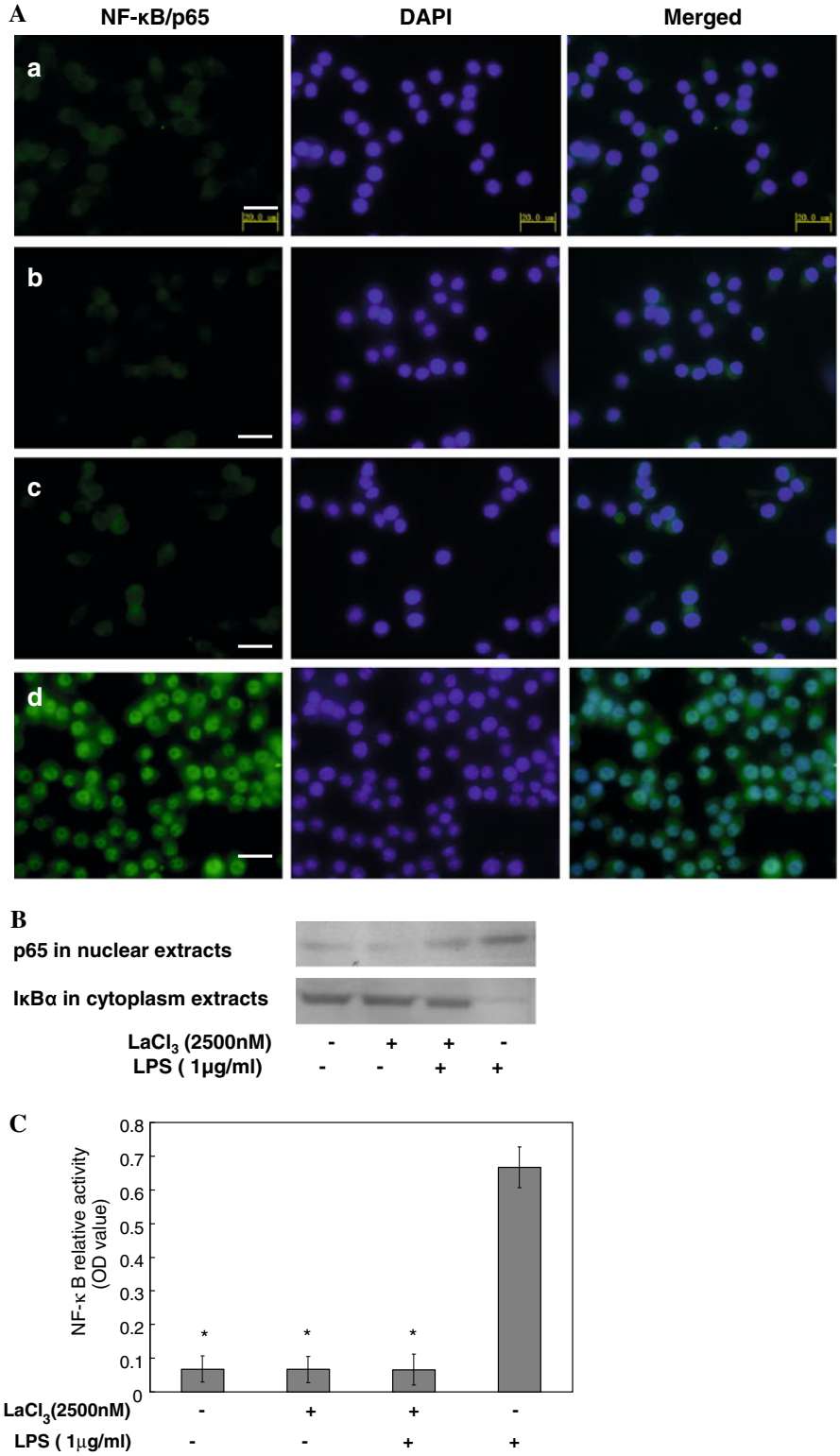

Fig. 5 Effect of lanthanum chloride on LPS-induced NF-κB activation in RAW 267.4 cells. **A** Immunofluorescent staining analysis of NF-κB/p65 protein: *a* control; *b* cells were treated with lanthanum chloride (2500 nM) in the absence of LPS for 30 min; *c* cells were pretreated with lanthanum chloride (2500 nM) for 2 h, washed, and stimulated with LPS (1 μg/ml) for 30 min; *d* cells were treated with LPS (1 μg/ml) for 30 min (*Bar* = 20 μm). **B** Total nuclear extracts and cytoplasm extracts were isolated and subjected to immunoblot analysis of NF-κB/p65 and IκBα, respectively. **C** Total nuclear extracts were isolated and used in an ELISA based NF-κB activity assay in which NF-κB is captured by a double-stranded DNA probe. * $P < 0.01$ vs. LPS alone

Lewis et al. 2005), and aurinetricarboxylic acid reduces the viability of AIDS virus by decreasing the DNA-binding activity of NF-κB intensively. Metals such as gold, palladium, nickel, and mercury regulate the activation of target gene by inhibiting the DNA-binding activity of NF-κB (Sharma et al. 2000).

It has been shown that NF-κB pathway is dependent on Ca^{2+}, i.e., the transcription of NF-κB is inositol triphosphate (InsP3)/Ca^{2+}-dependent (Valdes et al. 2007). To address the mechanisms by which lanthanum chloride blocks NF-κB and PKC activation, we detected $[Ca^{2+}]_i$ using Fluo-3/acetoxymethyl ester (Fluo-3/AM) by flow cytometry. We found that both $LaCl_3$ and extracellular/intracellular Ca^{2+} chelators blunted the LPS-induced increase in $[Ca^{2+}]_i$ significantly. According to Chang et al. (2008b), a bulk cytoplasmic Ca^{2+} signal might trigger the phosphorylation of PKCα, but the Ca^{2+} has to reach a certain level to stimulate the enzymes. On the basis of the abovementioned facts, we believe that a Ca^{2+} signaling pathway is primarily responsible for blocking the transcription of NF-κB.

In the present study, we demonstrated that lanthanum chloride exhibits anti-inflammatory activity through the inhibition of inflammatory mediators such as NO and TNF-α at gene transcription levels in LPS-activated RAW 264.7 cells. Furthermore the anti-inflammatory properties of lanthanum chloride were mediated via the inhibition of PKC α phosphorylation in the cytosol and subsequently of NF-κB activation in nucleus. Further studies to pinpoint the signaling molecules affected by lanthanum in IKK signaling are currently undertaken.

Lanthanum, a representative of lanthanides with extremely active physical and chemical properties was reported to possess antibacterial effect and can regulate cellular immunity. The toxicity of lanthanum is lower than that of synthetic drugs and some transition metals. For these reasons, lanthanides have already been employed as diagnostic agents in clinical examinations such as magnetic resonance imaging, time-resolved fluorescence immunoassays, and radioactive isotopic labeling. Besides, lanthanide compounds are also applied in the treatment of various diseases (Deveci et al. 2000; Hadjiiski and Lesseva 1999). For example, lanthanum carbonate is well tolerated and effective for the long-term maintenance of serum phosphorus control in patients with end-stage renal disease (Chiang et al. 2005). In addition, studies have also demonstrated great efficacy of sulfadiazine combined with cerium nitrate in the treatment of burn patients (Shigematsu 2008). Therefore, it is of great translational utility to demonstrate in this study that lanthanum chloride is a potent inhibitor of LPS-induced NO and TNF-α production via blocking PKC and NF-κB activation in macrophages. These findings suggest that lanthanum chloride could be a potential therapeutic agent for use in the treatment of various inflammatory diseases.

Acknowledgements The work was supported by the National Natural Science Foundation of China (30660182, 30960405), Natural Science Foundation of Jiangxi Province (2007GZ Y1132) and Program for Innovative Research Team of Nanchang University.

References

Baeuerle PA (1998) IkappaB-NF-kappaB structures: at the interface of inflammation control. Cell 95(6):729–731

Chang HT, Huang CC, Cheng HH, Wang JL, Lin KL, Hsu PT, Tsai JY, Liao WC, Lu YC, Huang JK, Jan CR (2008a) Mechanisms of AM404-induced [Ca(2+)](i) rise and death in human osteosarcoma cells. Toxicol Lett 179(1): 53–58

Chang WC, Di Capite J, Singaravelu K, Nelson C, Halse V, Parekh AB (2008b) Local Ca2+ influx through Ca2+ release-activated Ca2+ (CRAC) channels stimulates production of an intracellular messenger and an intercellular pro-inflammatory signal. J Biol Chem 283(8):4622–4631

Chen CC, Wang JK (1999) p38 but not p44/42 mitogen-activated protein kinase is required for nitric oxide synthase induction mediated by lipopolysaccharide in RAW 264.7 macrophages. Mol Pharmacol 55(3):481–488

Chen F, Sun SC, Kuh DC, Gaydos LJ, Demers LM (1995) Essential role of NF-kappa B activation in silica-induced inflammatory mediator production in macrophages. Biochem Biophys Res Commun 214(3):985–992

Chen C, Chen YH, Lin WW (1999) Involvement of p38 mitogen-activated protein kinase in lipopolysaccharide-induced iNOS and COX-2 expression in J774 macrophages. Immunology 97(1):124–129

Chiang SS, Chen JB, Yang WC (2005) Lanthanum carbonate (Fosrenol) efficacy and tolerability in the treatment of hyperphosphatemic patients with end-stage renal disease. Clin Nephrol 63(6):461–470

Choi DY, Toledo-Aral JJ, Segal R, Halegoua S (2001) Sustained signaling by phospholipase C-gamma mediates nerve growth factor-triggered gene expression. Mol Cell Biol 21(8):2695–2705

Dai J, Li CL, Zhang YZ, Xiao Q, Lei KL, Liu Y (2008a) Bioenergetic investigation of the effects of La(III) and Ca(II) on the metabolic activity of *Tetrahymena thermophila* BF5. Biol Trace Elem Res 122(2):148–156

Dai J, Zhang YZ, Liu Y, Li QG (2008b) Microcalorimetric study of the effect of Ce(III) on metabolic activity of mitochondria isolated from indice rice 9311. Chem Biodivers 5(7):1321–1326

De Broe ME (2008) Can the risk of gadolinium be extrapolated to lanthanum? Semin Dial 21(2):142–144

de Gracia CG (2001) An open study comparing topical silver sulfadiazine and topical silver sulfadiazine-cerium nitrate in the treatment of moderate and severe burns. Burns 27(1):67–74

Deveci M, Eski M, Sengezer M, Kisa U (2000) Effects of cerium nitrate bathing and prompt burn wound excision on IL-6 and TNF-alpha levels in burned rats. Burns 26(1):41–45

Fujii Y, Goldberg P, Hussain SN (1998) Contribution of macrophages to pulmonary nitric oxide production in septic shock. Am J Respir Crit Care Med 157(5 Pt 1):1645–1651

Ghosh S, Karin M (2002) Missing pieces in the NF-kappaB puzzle. Cell 109(Suppl):S81–S96

Hadjiiski OG, Lesseva MI (1999) Comparison of four drugs for local treatment of burn wounds. Eur J Emerg Med 6(1):41–47

Hambleton J, McMahon M, DeFranco AL (1995) Activation of Raf-1 and mitogen-activated protein kinase in murine macrophages partially mimics lipopolysaccharide-induced signaling events. J Exp Med 182(1):147–154

Hofmann J (1997) The potential for isoenzyme-selective modulation of protein kinase C. Faseb J 11(8):649–669

Hu J, Yu S, Yang X, Wang K, Qian Z (2006) Lanthanum induces extracellular signal-regulated kinase phosphorylation through different mechanisms in HeLa cells and NIH 3T3 cells. Biometals 19(1):13–18

Jeon KI, Byun MS, Jue DM (2003) Gold compound auranofin inhibits IkappaB kinase (IKK) by modifying Cys-179 of IKKbeta subunit. Exp Mol Med 35(2):61–66

Kao JP, Harootunian AT, Tsien RY (1989) Photochemically generated cytosolic calcium pulses and their detection by fluo-3. J Biol Chem 264(14):8179–8184

Lallena MJ, Diaz-Meco MT, Bren G, Paya CV, Moscat J (1999) Activation of IkappaB kinase beta by protein kinase C isoforms. Mol Cell Biol 19(3):2180–2188

Letari O, Nicosia S, Chiavaroli C, Vacher P, Schlegel W (1991) Activation by bacterial lipopolysaccharide causes changes in the cytosolic free calcium concentration in single peritoneal macrophages. J Immunol 147(3): 980–983

Lewis JB, Wataha JC, McCloud V, Lockwood PE, Messer RL, Tseng WY (2005) Au(III), Pd(II), Ni(II), and Hg(II) alter NF kappa B signaling in THP1 monocytic cells. J Biomed Mater Res A 74(3):474–481

Li S, Huang F, Feng Q, Liu J, Fan S, McKenna T (1998) Overexpression of protein kinase C alpha enhances lipopolysaccharide-induced nitric oxide formation in vascular smooth muscle cells. J Cell Physiol 176(2):402–411

Lin MQ, Chang ZL (1996) LPS and PMA induced PKC-alpha and PKC-epsilon activation and translocation in murine peritoneal macrophages. Shi Yan Sheng Wu Xue Bao 29(4):429–434

Manolov I, Raleva S, Genova P, Savov A, Froloshka L, Dundarova D, Argirova R (2006) Antihuman immunodeficiency virus type 1 (HIV-1) activity of rare earth metal complexes of 4-hydroxycoumarins in cell culture. Bioinorg Chem Appl 2006:71938

Moscat J, Diaz-Meco MT, Rennert P (2003) NF-kappaB activation by protein kinase C isoforms and B-cell function. EMBO Rep 4(1):31–36

Nahrevanian H, Dascombe MJ (2002) Expression of inducible nitric oxide synthase (iNOS) mRNA in target organs of lethal and non-lethal strains of murine malaria. Parasite Immunol 24(9–10):471–478

Nelson DE, Ihekwaba AE, Elliott M, Johnson JR, Gibney CA, Foreman BE, Nelson G, See V, Horton CA, Spiller DG, Edwards SW, McDowell HP, Unitt JF, Sullivan E, Grimley R, Benson N, Broomhead D, Kell DB, White MR (2004) Oscillations in NF-kappaB signaling control the dynamics of gene expression. Science 306(5696):704–708

Ogata N, Yamamoto H, Kugiyama K, Yasue H, Miyamoto E (2000) Involvement of protein kinase C in superoxide anion-induced activation of nuclear factor-kappa B in human endothelial cells. Cardiovasc Res 45(2):513–521

Oh PS, Lee SJ, Lim KT (2007) Glycoprotein isolated from *Rhus verniciflua* Stokes inhibits inflammation-related protein and nitric oxide production in LPS-stimulated RAW 264.7 cells. Biol Pharm Bull 30(1):111–116

Parker PJ, Murray-Rust J (2004) PKC at a glance. J Cell Sci 117(Pt 2):131–132

Qin JF, Chen XY, Li ZX (2002) Biological effect of rare earth element. Guang Dong Wei Liang Yuan Su Ke Xue 9(5):1–10

Roland CR, Naziruddin B, Mohanakumar T, Flye MW (1996) Gadolinium chloride inhibits Kupffer cell nitric oxide synthase (iNOS) induction. J Leukoc Biol 60(4):487–492

Sanghera JS, Weinstein SL, Aluwalia M, Girn J, Pelech SL (1996) Activation of multiple proline-directed kinases by bacterial lipopolysaccharide in murine macrophages. J Immunol 156(11):4457–4465

Severn A, Wakelam M, Liew F (1992) The role of protein kinase C in the induction of nitric oxide synthesis by murine macrophages. Biochem Biophys Res Commun 188(3):997–1002

Sharma RK, Garg BS, Kurosaki H, Goto M, Otsuka M, Yamamoto T, Inoue J (2000) Aurine tricarboxylic acid, a potent metal-chelating inhibitor of NFkappaB-DNA binding. Bioorg Med Chem 8(7):1819–1823

Shigematsu T (2008) Lanthanum carbonate effectively controls serum phosphate without affecting serum calcium levels in patients undergoing hemodialysis. Ther Apher Dial 12(1):55–61

Spitaler M, Cantrell DA (2004) Protein kinase C and beyond. Nat Immunol 5(8):785–790

Steffan NM, Bren GD, Frantz B, Tocci MJ, O'Neill EA, Paya CV (1995) Regulation of IkB alpha phosphorylation by PKC- and Ca(2+)-dependent signal transduction pathways. J Immunol 155(10):4685–4691

Sudhandiran G, Shaha C (2003) Antimonial-induced increase in intracellular Ca2 + through non-selective cation channels in the host and the parasite is responsible for apoptosis of intracellular Leishmania donovani amastigotes. J Biol Chem 278(27):25120–25132

Trushin SA, Pennington KN, Carmona EM, Asin S, Savoy DN, Billadeau DD, Paya CV (2003) Protein kinase Calpha

(PKCalpha) acts upstream of PKCtheta to activate IkappaB kinase and NF-kappaB in T lymphocytes. Mol Cell Biol 23(19):7068–7081

Valdes JA, Hidalgo J, Galaz JL, Puentes N, Silva M, Jaimovich E, Carrasco MA (2007) NF-kappaB activation by depolarization of skeletal muscle cells depends on ryanodine and IP3 receptor-mediated calcium signals. Am J Physiol Cell Physiol 292(5):C1960–C1970

Wang Y, Guo F, Hu F, Wang G, Li G (2004) Lanthanum inhibited the binding of LPS with monocyte and CD 14 expression upregulation. Cell Mol Immunol 1(5):392–394

Wolfs TG, Buurman WA, van Schadewijk A, de Vries B, Daemen MA, Hiemstra PS, van 't Veer C (2002) In vivo expression of Toll-like receptor 2 and 4 by renal epithelial cells: IFN-gamma and TNF-alpha mediated up-regulation during inflammation. J Immunol 168(3):1286–1293

Xie QW, Kashiwabara Y, Nathan C (1994) Role of transcription factor NF-kappa B/Rel in induction of nitric oxide synthase. J Biol Chem 269(7):4705–4708

Zhang P, Martin M, Michalek S, Katz J (2005) Role of mitogen-activated protein kinases and NF-κB in the regulation of proinflammatory and anti-inflammatory cytokines by *Porphyromonas gingivalis*. Hemagglutinin B Infect Immun 73(7):3990–3998

Zhong H, SuYang H, Erdjument-Bromage H, Tempst P, Ghosh S (1997) The transcriptional activity of NF-kappaB is regulated by the IkappaB-associated PKAc subunit through a cyclic AMP-independent mechanism. Cell 89(3):413–424

Zhu Y, Gu ZL, Liang ZQ, Zhang HL, Qin ZH (2006) Prostaglandin A1 inhibits increases in intracellular calcium concentration, TXA(2) production and platelet activation. Acta Pharmacol Sin 27(5):549–554